Journal of Non-Crystalline Solids 637 (2024) 123046

Contents lists available at ScienceDirect

Journal of Non-Crystalline Solids

journal homepage: www.elsevier.com/locate/jnoncrysol

Colossal low-temperature upturn in the heat capacity of volcanic glasses

Daria Szewczyk [a,b,*], Michele Cassetta [c,d,*]

[a] Department of Low Temperature and Superconductivity, Institute of Low Temperature and Structure Research PAS, 50-422, Wroclaw, Poland
[b] Departamento de Física de la Materia Condensada & Instituto "Nicolás Cabrera", Universidad Autónoma de Madrid, 28049 Madrid, Spain
[c] Department of Industrial Engineering, University of Trento, I-38122 Trento, Italy
[d] Department of Engineering for Innovation Medicine, University of Verona, I-37134 Verona, Italy

ARTICLE INFO

Keywords:
Volcanic glasses
Low-temperature heat capacity

ABSTRACT

Here we explore the low-temperature heat capacity (C_p) of two natural endmember volcanic glasses, unveiling an unprecedented anomalous upturn in C_p/T^3 versus temperature (T) dependencies. This distinctive behavior, previously unseen at this scale, obscures the accurate boson peak position, posing a significant analytical challenge. Through rigorous examination, we established the magnetic origin of this anomaly, proved by subjecting the samples to a magnetic field up to 9 Tesla. The investigations uncovered a nuanced interplay between magnetic models, as we sought to provide an explanation for describing this captivating phenomenon.

1. Introduction

The mechanisms governing the eruptive style of volcanoes are deeply connected to the physicochemical properties of magmas. These materials are usually classified as multiphase and multicomponent systems, whose structure controls the dynamics of the magmatic rising [1]. The liquid phase of these systems represents their leading component dominating viscoelastic response and flow behavior [2]. Any magmatic process is unavoidably recorded into the silicate structures of the erupted products and in particular, the glassy fraction records the final moments of an eruption. Following, the study of these enigmatic glasses opened the way to a wide range of methodologies aimed at unveiling their intrinsic structure (*i.e.* short and medium range order) and how it affects their macroscopic response to deformations [3–5]. However, still little is known about their low-temperature heat capacity (C_p). Indeed, its temperature dependence is key in accessing the glass structure and, paradoxically, the high-temperature entropy thus, underpinning deep implications on melt viscosity [6]. Following, the exploration of low-T range of simplified silicate glassy systems suggests that C_p is mostly governed by variations of the structural medium-range order rather than by an additive compositional law [7–9]. However, those investigations were conducted by ruling out an essential component of natural silicate glass: iron. Despite the numerous approaches and methodologies used to unravel its intriguing behavior, the role of iron in the medium- and short-range order of silicate glasses is and remains a standing issue [10]. Here we provide strong evidences of its potential magnetic influence displayed by a colossal low-T upturn in two end-member natural volcanic glasses: basalt and rhyolite respectively. This anomaly has never been observed or reported in literature in silicate glasses so far. Thus, we also attempted an interpretation of our preliminary results in terms of an additional spin fluctuation contribution [11] or cluster theory [12,13], obtaining a surprising competition between the two approaches in describing the heat capacity data of both samples subjected to a magnetic field.

2. Materials and methods

The investigated volcanic glasses (characterized in Ref. [14,15]) represent two natural sub-alkaline endmembers, basalt (B_{100}) and rhyolite (R_{100}) respectively, whose composition, $Fe^{2+}/Fe_{tot.}$ ratio and densities (ρ) are reported in Table 1. The two glasses differ mainly from their content in SiO_2, and the most relevant element-oxides of the so-called network modifiers group (CaO, MgO, Na_2O, K_2O) and particularly in FeO_{tot}. B_{100} is richer in non-bridging oxygen and iron oxide than R_{100} that shows a much stronger network-connectivity. According to the Raman spectra reported in [15] the R_{100} structure is richer in larger tetrahedral rings (*i.e.* 6-membered rings) with respect to that of B_{100}.

Temperature dependence of heat capacity was determined by a standard thermal relaxation method implemented in the He^4 PPMS system [16]. The measurements were taken for a temperature range from 1.9 K up to 50 K with the magnetic field from 0T to 9T in 1T step.

* Corresponding authors.
E-mail addresses: d.szewczyk@intibs.pl (D. Szewczyk), michele.cassetta@univr.it (M. Cassetta).

https://doi.org/10.1016/j.jnoncrysol.2024.123046
Received 25 November 2023; Received in revised form 20 May 2024; Accepted 22 May 2024

The mass of particular samples used in the experiment was: B_{100}–10.70 mg and R_{100}–8.45 mg.

3. Results and discussions

The characteristics of the low temperature heat capacity of glasses are a linear term contribution and the appearance of the boson peak (BP) which is a result of an excess in the low-frequency THz of the vibrational density of states, universally related to the intrinsic disorder of glasses (see the BP of SiO_2 glass in Fig. 1). The experimental data can be accordingly approximated according to Ref. [17] as:

$$C_p = \alpha T + \beta T^3 + \delta T^5, \quad (1)$$

where αT corresponds to the tunneling between two level states, βT^3 is the Debye contribution present in any solid and δT^5 stems from the soft modes. For a typical C_p/T^3 vs T one should expect a pronounced maximum at the BP temperature and depending on the available temperature range towards the low temperatures an upturn related to the linear term in the Eq. (1). Fig. 1 shows the raw C_p/T^3 vs T results for the R_{100} and B_{100}. In order to emphasize the expected traditional glassy picture (BP), the literature data of SiO_2 case are included as solid grey lines [18,19]. The inset in upper left corner shows the experimental data in C_p/T vs T^2 coordinates up to 10 K range.

The BP vicinity is almost undetectable in both volcanic glasses, in R_{100} BP (although very smeared) is still determinable, whilst in B_{100} it is no longer possible. In order to eliminate the unlikely experimental system's influence, additional runs confirming the high accuracy and repeatability of specific heat data, further measurements were performed on a secondary calorimetric cell (not included in the paper) for both samples.

It can be inferred that the real behavior at the lowest temperatures is hidden by a massive contribution from the low temperature range, associated with the linear contribution. To present the enormous extent of this anomalous behavior at lowest temperatures, an additional plot showing the higher values at the Y axis is reported in *Supplementary material*, Figure S1. The distinct temperature dependence is even more pronounced when the experimental data are plotted in the C_p/T vs T^2 form (see inset in Fig. 1). Instead of a simple linear dependence (or lightly parabolic if the soft potential model in the C_p approximation is included) we report a strong "upturn" at temperatures below 4.5 K for R_{100} and 9 K for B_{100}. A direct example of this behavior is reported in Ref. [20], where an iron bearing soda-lime glass, loaded with 2 wt.% of Fe_2O_3 shows a quite similar behavior of our R_{100}, which is not surprising being quite similar in structure and composition. Moreover, the behavior of a Pyrex glass with 0.02 wt.% of FeO (considered as impurity) [21], shows a magnetic field dependence similar to our B_{100} displaying a threshold field above 2T but again, without any low-temperature upturn worth of note. Thus, such a behavior, in particular that of B_{100}, has not been documented in any silicate systems to date.

Nevertheless, such low-T upturn, was seen only in alloys and materials exhibiting ferromagnetism [22–24] and described by means of either spin fluctuation [11] or magnetic clusters [12,13]. In order to confirm that the peculiar behavior is of magnetic origin, the field dependence of the heat capacity of R_{100} and B_{100} was studied in detail. The results from the tests with magnetic fields (up to 9 T), are presented in Fig. 2.

Fig. 2 shows the magnetic field influence on the low temperature heat capacity of studied volcanic glasses. In both cases one can determine the initial enhancement of the additional, excess contribution to the specific heat with an increasing magnetic field up to a certain threshold value, different for each glass. In the case of B_{100}, the initial subjection of the sample to 1T and 2T magnetic field results in an increased anomaly at low temperatures, while further increasing of the external field gradually softens the phenomena. R_{100} also shows the strongest enhancement of the behavior for a 1T and 2T field, while in this case only 5T field addition to the sample results in a final decrease of the excess heat capacity contribution. The field influence on the heat capacity was indicated by directional arrows on plots tracking the evolution of anomaly (Fig. 2). Given the above magnetic field dependence one can conclude that the anomalous C_p cannot be described within a standard disordered system approach, Eq. (1), but one should include other terms related to the magnetic contributions. Additional indications for looking beyond the standard approach are given also in Figure S2 of *Supplementary Material*, where the reduced heat capacity data still exhibits a low-T upturn. Looking at the composition of those multicomponent glasses, Table 1, (ten different oxides), sounds reasonable to ascribe this peculiar magnetically induced behavior to Fe ions. For this possible explanation the additional arguments in favor could be given by simply looking at the absolute values of heat capacity in Fig. 2. The *colossal low-T upturn* in the case of the B_{100} is almost 4 times higher than that of R_{100} which corresponds to the increased Fe content in the sample. The accurate description of the magnetic contributions to the low-T heat capacity should include two approaches:

(*i*) extension of the conventional Eq. (1), by including the spin wave ($B_{3/2}T^{3/2}$) and hyperfine $\left(\frac{\varepsilon}{T^2}\right)$ contributions, [25,26]

$$C_p = \frac{\varepsilon}{T^2} + B_{3/2}T^{3/2} + \gamma T + \beta T^3. \quad (2)$$

Another significant point here is that the linear term also includes the

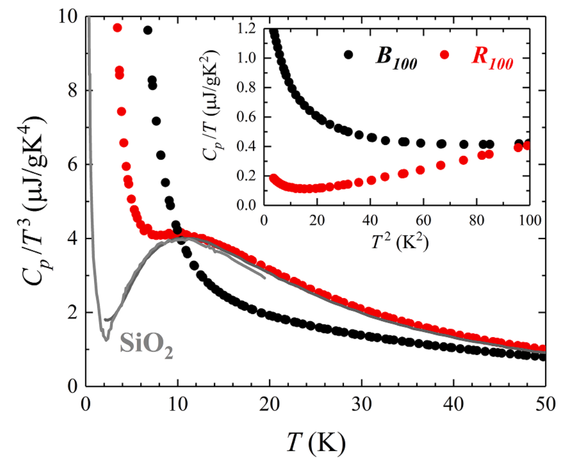

Fig. 1. C_p/T^3 *vs.* T plots of basaltic (B_{100}) and rhyolitic (R_{100}) volcanic glasses together with pure silica glass (SiO_2) from Ref. [18]. Inset: C_p/T *vs.* T^2 plot of volcanic glasses B_{100} and R_{100}.

Table 1
Chemical composition in wt.%, total iron oxide ($FeO_{tot.}$), the ratio between ferrous and total iron cations ($Fe_{tot.}$) expressed as $Fe^{2+}/Fe_{tot.}$ and density (ρ) of basaltic (B_{100}) and rhyolitic (R_{100}) glasses from Ref. [14].

	SiO_2	TiO_2	Al_2O_3	$FeO_{tot.}$	MnO	MgO	CaO	Na_2O	K_2O	P_2O_5	$Fe^{2+}/Fe_{tot.}$	ρ [g cm^{-3}]
B_{100}	49.71	0.76	9.51	8.86	0.16	14.53	14.64	1.80	0.03	0.01	0.386	2.757
R_{100}	79.82	0.10	8.57	1.86	0.07	0.71	1.57	3.92	3.37	0.01	0.342	2.368

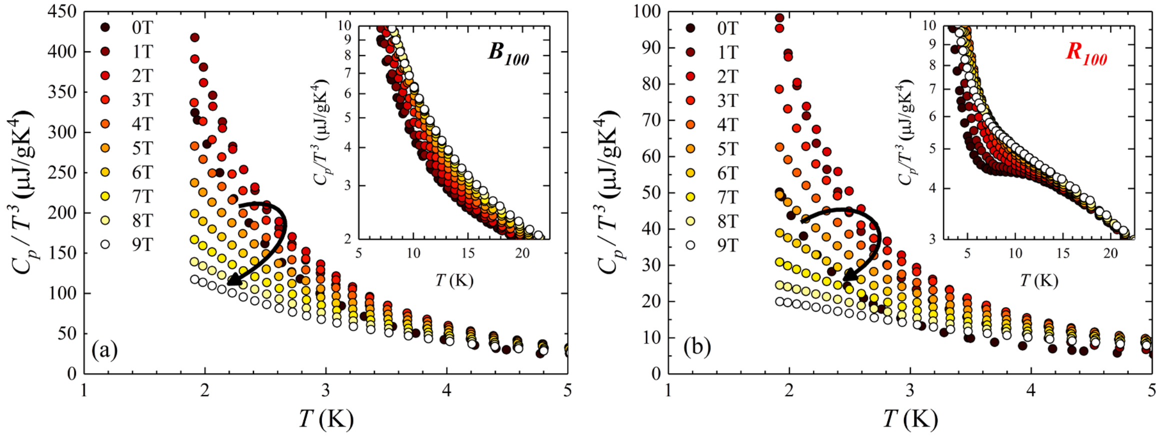

Fig. 2. Field dependent C_p/T^3 *vs.* T plots of volcanic glasses B_{100}, the basalt (a) and R_{100}, the rhyolite (b). Insets show a broader temperature range field influence.

electronic contribution to low-T heat capacity and there is no simple way to extract each of them.

(*ii*) the anomalous low-T heat capacity is the result of magnetic clusters. Here, an additional term is introduced as the excess heat capacity [23],

$$C_{excess} = A_0\left[E\left(\frac{\theta_S}{T}\right) - E\left(\frac{N_e\theta_S}{T}\right)\right], \quad (3)$$

where $E(x) = x^2e^x(e^x-1)^{-2}$ is Einstein function, $A_0 = N_c{\cdot}k_B$, N_c is the number of clusters, defined as Fe-rich regions, $\theta_S = \varepsilon / k_B$, with ε is the energy between the levels, and their number (N_e) [23].

In order to accurately describe the volcanic glasses data at different magnetic fields, both of the approximations were tested. In the case of the first approach – Eq. (2), the fits were introduced as short dotted lines on the plots of particular fields of Fig. 3. In the second approach, according to the magnetic clusters model, the fits are given by solid lines following the equation:

$$\frac{C_p}{T} = \frac{\alpha + \beta T^2 + A_0\left[E\left(\frac{\theta_S}{T}\right) - E\left(\frac{N_e\theta_S}{T}\right)\right]}{T}. \quad (4)$$

The output values of the fitting parameters of Eqs. (2) and (4) are reported in Table S1 and S2 in the *Supplementary material*. In both cases the C_p was approximated disregarding the T^5 - soft modes term, as one with a very minor impact on the resulting heat capacity.

The Fig. 3 includes all applied fields in the case of B_{100} (with higher Fe content) whilst the resulting plots of the R_{100} sample are given in Fig. 4. The map of separate panels for each magnetic field was designed to visualize the changing behavior in samples.

The plots of Fig. 3 and Fig. 4 clearly show a competition-like between

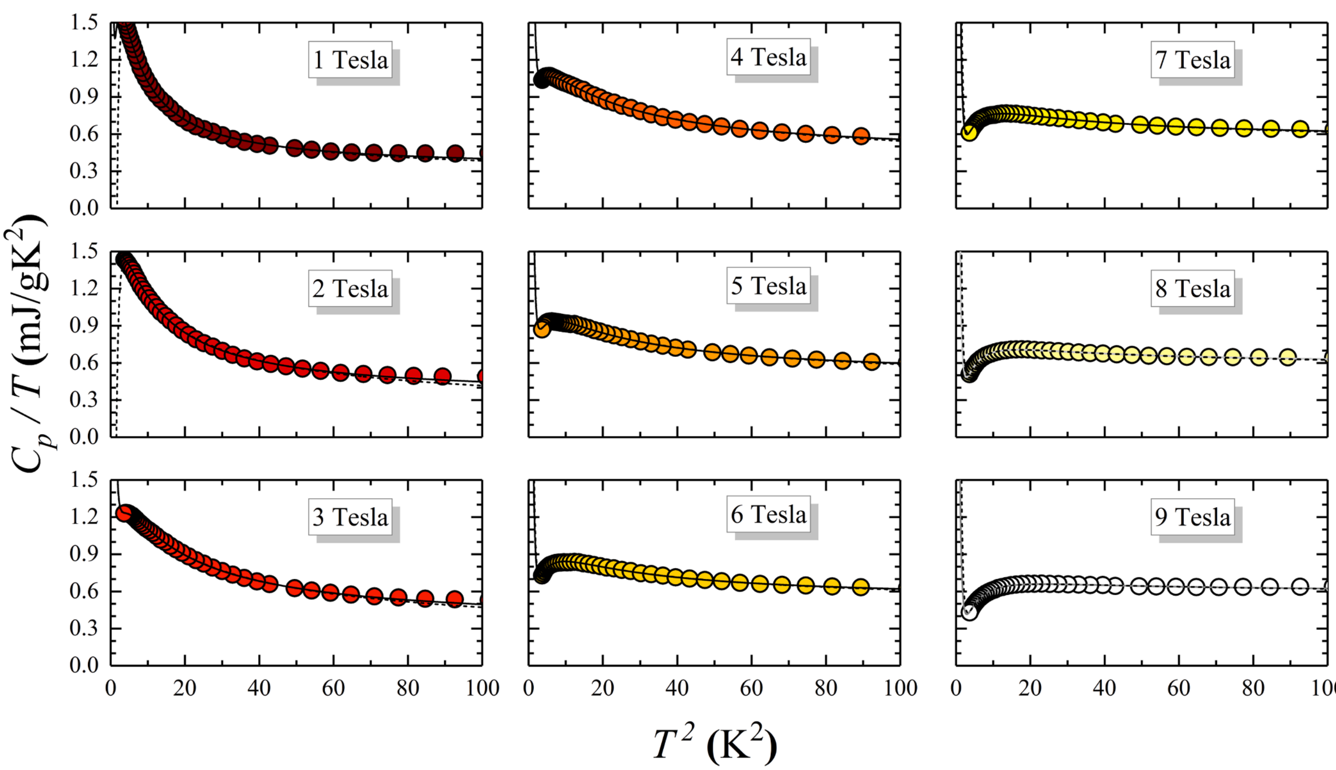

Fig. 3. The fitted C_p/T *vs.* T^2 plots of the basaltic glass (B_{100}) obtained under different magnetic fields.

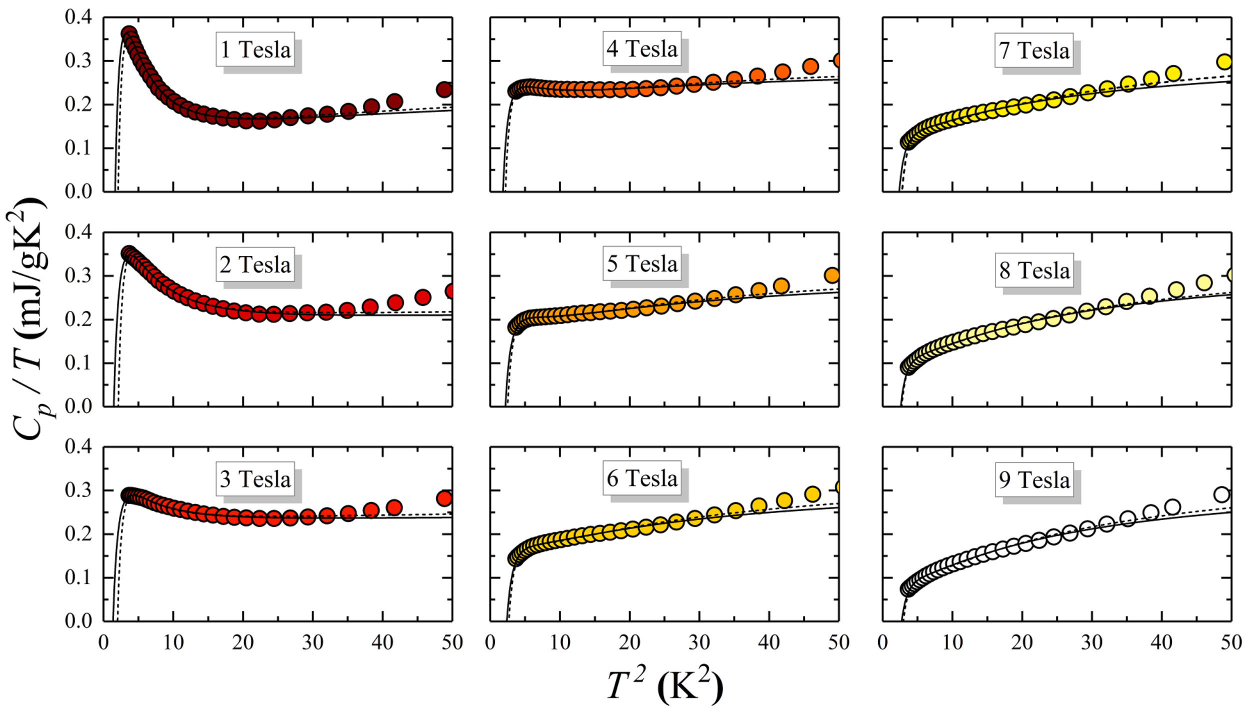

Fig. 4. The fitted C_p/T *vs.* T^2 plots of the rhyolitic glass R_{100} obtained under different magnetic fields.

the models Eqs. (2) and (4) in describing the two samples (see the dotted and solid lines respectively). One can almost claim that both fits work equally well as would be expected in temperatures well below the possible BP of the studied materials. In the case of the B_{100} sample the experimental data were approximated with each model below 70–75K^2 $\approx$ 8.5 K, for the R_{100} one, the fitting region was limited to temperatures below 35–40K^2 $\approx$ 6 K. The observed C_p/T^3 curves (Fig. 2) of the threshold magnetic field saturating at 2T, can also be traced on Fig. 3 and Fig. 4, and directly in the used approximation. Looking closely at output parameters of Eqs. (2) and (4), Table S1 and S2, one finds corresponding trends of particular values following the magnetic field dependence. Namely, an initial enhancement of anomalous behavior up to 2T for B_{100} and R_{100} is matching either decrease or increase of fitting parameters, followed by the reverse trend after overcoming the field threshold value, 5T for B_{100} and 3T for R_{100} respectively. Moreover, it is important to mention that only in the case of B_{100} the magnetic clusters model provided the physical parameters giving clues on the magnetic behavior standing behind the observed phenomena. In all the remaining examples, the approximation matches the experimental data with high accuracy but lacks scientific justification.

To better visualize the magnetic field evolution with the related fits we provided two gifs in the *Supplementary material*, Figure S3 and S4. Once more, including the above presented analysis we emphasize that this complex magnetic nature of investigated volcanic glasses cannot be attributed to only one particular mechanism.

4. Conclusions

Contrary to expectations, a colossal upturn at low temperature heat capacity was observed for both investigated volcanic glasses: basaltic (B_{100}) and rhyolitic (R_{100}). As a result, a conventional disordered structure approximation of the experimental data was not applicable. It revealed the existence of an excess phenomena of magnetic origin, and motivated additional studies with magnetic field dependence up to 9T. The excess heat capacity was accurately described within the known magnetic models, but the observed magnetic behavior and hence the origin of the colossal upturn was found to be of complex origin and could not be straightforwardly assigned to only one type of mechanism (*i.e.* fluctuating spin or iron-rich clusters). In order to define the exact applicability ranges of the approximations, advanced further studies, including magnetization and susceptibility are necessary. Finally, we outline that low-T heat capacity studies offers a potentially promising and integrative approach to determine the contribution of magnetic elements in volcanic glasses (iron), in addition to its application in assessing the medium-range order of glass and possibly to provide new insights on the nucleation of nanometric iron-bearing oxides crystals.

CRediT authorship contribution statement

Daria Szewczyk: Writing – original draft, Validation, Methodology, Investigation, Formal analysis, Conceptualization. **Michele Cassetta:** Writing – review & editing, Visualization, Resources, Investigation, Conceptualization.

Declaration of competing interest

The authors declare that they have no known competing financial interests or personal relationships that could have appeared to influence the work reported in this paper.

Data availability

Data will be made available on request.

Acknowledgement

We warmly acknowledge F. Vetere and G. Iezzi for providing samples, as well as L. Bastianelli for his precious graphical support.

Supplementary materials

Supplementary material associated with this article can be found, in the online version, at doi:10.1016/j.jnoncrysol.2024.123046.

References

[1] D.B. Dingwell, S.L. Webb, Structural relaxation in silicate melts and non-Newtonian melt rheology in geologic processes, Phys. Chem. Miner. 16 (1989) 508–516, https://doi.org/10.1007/BF00197020.

[2] H.M. Gonnermann, M. Manga, The fluid mechanics inside a volcano, Annu. Rev. Fluid Mech. 39 (2007) 321–356, https://doi.org/10.1146/annurev.fluid.39.050905.110207.

[3] M. Cassetta, G. Mariotto, N. Daldosso, E. De Bona, M. Biesuz, G.D. Sorarù, R. Almeev, M. Zanatta, F. Vetere, Viscosity, boson peak and elastic moduli in the Na_2O-SiO_2 system, Minerals 13 (2023) 1166, https://doi.org/10.3390/min13091166.

[4] M. Wilke, Fe in magma - an overview, Ann. Geophys. 48 (2005) 609–617, https://doi.org/10.4401/ag-3222.

[5] P.A. Bingham, J.M. Parker, T. Searle, J.M. Williams, K. Fyles, Redox and clustering of iron in silicate glasses, J. Non. Cryst. Solids 253 (1999) 203–209, https://doi.org/10.1016/S0022-3093(99)00361-0.

[6] P. Richet, R.A. Robie, B.S. Hemingway, Low-temperature heat capacity of diopside glass ($CaMgSi_2O_6$): a calorimetric test of the configurational-entropy theory applied to the viscosity of liquid silicates, Geochim. Cosmochim. Acta 50 (1986) 1521–1533, https://doi.org/10.1016/0016-7037(86)90326-1.

[7] J. Majzlan, J.A. Tangeman, E. Dachs, Heat capacity, entropy, configurational entropy, and viscosity of magnesium silicate glasses and liquids, Phys. Chem. Miner. 48 (2021) 1–11, https://doi.org/10.1007/s00269-021-01153-7.

[8] D. De Ligny, E.F. Westrum, Entropy of calcium and magnesium aluminosilicate glasses, Chem. Geol. 128 (1996) 113–128, https://doi.org/10.1016/0009-2541(95)00167-0.

[9] P. Richet, R.A. Robie, B.S. Hemingway, Entropy and structure of silicate glasses and melts, Geochim. Cosmochim. Acta 57 (1993) 2751–2766, https://doi.org/10.1016/0016-7037(93)90388-D.

[10] M. Cassetta, B. Giannetta, F. Enrichi, C. Zaccone, G. Mariotto, M. Giarola, L. Nodari, M. Zanatta, N. Daldosso, Effect of the alkali vs iron ratio on glass transition temperature and vibrational properties of synthetic basalt-like glasses, Spectrochim. Acta - Part A Mol. Biomol. Spectrosc. 293 (2023) 122430, https://doi.org/10.1016/j.saa.2023.122430.

[11] K. Ikeda, S.K. Dhar, M. Yoshizawa, K.A. Gschneidner, Quenching of spin fluctuations by high magnetic fields, J. Magn. Magn. Mater. 100 (1991) 292–321, https://doi.org/10.1016/0304-8853(91)90826-V.

[12] A. Hahn, E.P. Wohlfarth, Anomalous low temperature specific heat of alloys near the critical concentration for ferromagnetism, Helv. Phys. Acta 41 (1968) 857.

[13] K. Schröder, C.H. Cheng, Correlation of low-temperature caloric and magnetic effects in Tife, J. Appl. Phys. 31 (1960) 2154–2155, https://doi.org/10.1063/1.1735515.

[14] F. Vetere, G. Iezzi, H. Behrens, F. Holtz, G. Ventura, V. Misiti, A. Cavallo, S. Mollo, M. Dietrich, Glass forming ability and crystallisation behaviour of sub-alkaline silicate melts, Earth-Sci. Rev. 150 (2015) 25–44, https://doi.org/10.1016/j.earscirev.2015.07.001.

[15] M. Cassetta, B. Rossi, S. Mazzocato, F. Vetere, G. Iezzi, A. Pisello, M. Zanatta, N. Daldosso, M. Giarola, G. Mariotto, Deep-UV Raman spectroscopy: a novel heuristic method to characterize volcanologically relevant glasses on Mars, Chem. Geol. 644 (2024) 121867, https://doi.org/10.1016/j.chemgeo.2023.121867.

[16] J.S. Hwang, K.J. Lin, C. Tien, Measurement of heat capacity by fitting the whole temperature response of a heat-pulse calorimeter, Rev. Sci. Instrum. 68 (1997) 94–101, https://doi.org/10.1063/1.1147722.

[17] M.A. Ramos, Low-temperature thermal and vibrational properties of disordered solids, 2022. https://doi.org/10.1142/q0371.

[18] R.C. Zeller, R.O. Pohl, Thermal conductivity and specific heat of non-crystalline solids, Phys. Rev. B 4 (1972) 2029–2041, https://doi.org/10.1016/0375-9601(72)90483-5.

[19] R.O. Pohl, Low temperature specific heat of glasses, Amorph. Solids (1981) 27–52, https://doi.org/10.1007/978-3-642-81534-8_3.

[20] N.G.C. Astrath, A. Steimacher, A.N. Medina, J.H. Rohling, J.R.D. Pereira, A. C. Bento, M.L. Baesso, L.M. da Silva, F.G. Gandra, Low temperature specific heat of doped and undoped glasses, J. Non Cryst. Solids 352 (2006) 3572–3576, https://doi.org/10.1016/j.jnoncrysol.2006.03.088.

[21] R.A. Fisher, G.E. Brodale, E.W. Hornung, W.F. Giauque, Thermal conductivity and heat capacity of 7740 pyrex below 4°K and in magnetic fields to 90 kG, Rev. Sci. Instrum. 39 (1968) 108–114, https://doi.org/10.1063/1.1683081.

[22] R.L. Falge, N.M. Wolcott, Cluster specific heats in copper-rich Cu-Ni alloys: the effect of iron, J. Low Temp. Phys. 5 (1971) 617–650, https://doi.org/10.1007/BF00628414.

[23] C. Wang, M. Palit, N. Yin, Q. Shi, Y. Ivanisenko, H. Gleiter, H. Hahn, Magnetic contributions to the low-temperature specific heat of $Sc_{79}Fe_{21}$ nanoglass, J. Appl. Phys. (2019) 125, https://doi.org/10.1063/1.5082579.

[24] E.S.R. Gopal, Magnetic contribution to specific heats, Specif. Heats Low Temp. 84 (1966) 84–111, https://doi.org/10.1007/978-1-4684-9081-7_5.

[25] V.K. Anand, D.T. Adroja, A.D. Hillier, Ferromagnetic cluster spin-glass behavior in $PrRhSn_3$, Phys. Rev. B - Condens. Matter Mater. Phys. 85 (2012) 1–9, https://doi.org/10.1103/PhysRevB.85.014418.

[26] X. Li, Y.Q. Cai, Q. Cui, C.J. Lin, Z.L. Dun, K. Matsubayashi, Y. Uwatoko, Y. Sato, T. Kawae, S.J. Lv, C.Q. Jin, J.S. Zhou, J.B. Goodenough, H.D. Zhou, J.G. Cheng, Long-range magnetic order in the Heisenberg pyrochlore antiferromagnets $Gd_2Ge_2O_7$ and $Gd_2Pt_2O_7$ synthesized under high pressure, Phys. Rev. B 94 (2016) 1–9, https://doi.org/10.1103/PhysRevB.94.214429.